Paradigm International Journal of Mathematics and Computer in Engineering 4(2) (2026) 281–292

International Journal of Mathematics and Computer in Engineering

https://reference-global.com/journal/IJMCE

Original Study

Groundwater depletion: A mathematical model incorporating climate and human factors

Kottakkaran Sooppy Nisar[1†], Raghad Mohammed Al-Suliman[1], Mada Samhoud Al-Qahtani[1]

[1]Department of Mathematics, College of Science and Humanities, Prince Sattam bin Abdulaziz University, Alkharj, 11942, Saudi Arabia

Communicated by Haci Mehmet Baskonus; Received: 15.12.2024; Accepted: 05.01.2026; Online: 02.06.2026

Abstract

Groundwater is vital for ecological balance and human use but is increasingly affected by factors such as pollution, excessive water consumption, and deforestation. We develop an advanced ordinary differential equation (ODE) model that includes new terms reflecting interactions between atmospheric water, surface water, and groundwater. This model incorporates various parameters for pollution, frequent water pumping, and deforestation, and examines how these factors influence groundwater dynamics. To investigate the system's behavior, we conduct a detailed analysis of equilibrium points and their stability. The model is further validated through numerical simulations by using the Runge-Kutta 4th order (RK4) method, which reveal the influence of various stressors on groundwater sustainability. This approach enhances understanding of groundwater interactions and supports better resource management strategies.

Keywords: Mathematical modelling, equilibrium points, stability results, numerical investigation.
AMS 2020 codes: 34D20; 76Z10; 65L07.

1 Introduction

Groundwater is an essential component of the Earth's water cycle, providing critical support for ecosystems, agriculture, and human consumption. It serves as a primary source of freshwater, especially in regions where surface water is scarce. However, groundwater resources are increasingly under pressure due to human activities such as over-extraction, pollution, and deforestation [1–5]. These environmental challenges disrupt the natural balance of groundwater replenishment, leading to long-term consequences such as depletion and contamination. Reports have highlighted the urgent need for effective groundwater management strategies, emphasizing the climate change's effects on water resources. However, existing models often lack detailed representations of the additional stresses imposed by human activities like pollution and deforestation [6–11]. In addition to traditional ODEs, the application of fractional calculus has gained traction in various fields, providing a framework to model procedures that display memory impacts and non-local behavior. Fractional models can capture the complexities of systems that are not well represented by classical integer-order models, allowing for more accurate predictions in scenarios influenced by historical states and environmental factors [12–19]. Recent research has also explored the controllability of such systems using advanced mathematical tools, such as fixed point theorems in Banach spaces, to analyze impulsive fractional

†Corresponding author.
Email address: ksnisar1@gmail.com

Paradigm
ISSN 2956-7068 doi:10.2478/ijmce-2026-0016 Paradigm

integro-differential equations, further extending the utility of fractional models in environmental and engineering applications [20]. Numerous studies have focused on developing mathematical models to describe the dynamics of groundwater systems. Researchers have employed ODE models to capture the interactions between atmospheric water, surface water, and groundwater [21–25]. These models help in understanding how various factors, including precipitation, evaporation, infiltration, and pumping, affect groundwater levels over time. However, existing models often lack detailed representations of the additional stresses imposed by human activities like pollution and deforestation. Previous researchers have made significant strides in modeling groundwater dynamics using ODEs. For instance, studies have incorporated key environmental processes such as evaporation, infiltration, and recharge into models to predict groundwater levels under various scenarios. Additionally, some studies have looked at how urbanization and climate change affect water cycles, shedding light on the potential impacts of these factors on groundwater systems [26–31]. These models serve as a foundation for developing strategies to manage groundwater resources more effectively. Moreover, water pollution stands out as a significant environmental challenge confronting developing nations. Mathematical modeling has proven effective in analyzing the transmission of water pollutants and their impact on ecosystems and public health. Numerical approaches, such as the use of shifted Jacobi polynomials, were also adopted to convert the model into an algebraic form and validate its performance against traditional Runge-Kutta methods [32]. In recent research, a system of ODEs was used to model soluble and insoluble pollutants, with sensitivity analysis performed on the reproduction number to assess intervention strategies [33]. These findings underscore the importance of integrating pollution dynamics into groundwater models to better reflect real-world complexities.

Building upon the existing ODE models, our research introduces additional terms to better capture the complex interactions between groundwater and environmental stressors. Specifically, we modify the standard ODE framework by incorporating terms for pollution, frequent water pumping, and deforestation. These new terms provide a more comprehensive representation of the factors affecting groundwater dynamics in modern contexts. Our work focuses on analyzing equilibrium points and stability while deriving numerical simulations to validate the model's performance across different environmental scenarios [34, 35]. By refining the ODE model and incorporating real-world factors, our approach offers deeper insights into groundwater behavior, making it a valuable tool for resource management and sustainability planning.

This study is structured as follows: Section 2 outlines the mathematical model's fundamental assumptions and parameter definitions. Section 3 details the system's equilibrium points. Section 4 examines the stability of these equilibrium points. In Section 5, we use numerical simulations to test the model and evaluate its behaviour in different environmental circumstances. Section 6 summarises the study's results and implications for managing groundwater resources. Section 7 completes the paper by presenting novelties of this work.

2 Model description

In this part of the paper, we present the model studied as follows

$$\begin{cases} \frac{dA}{dt} = \rho_1 B(t) + \rho_2 C(t) - \varpi A(t) - \iota A(t) + \kappa \frac{B(t)}{C(t)+1}, \\ \frac{dB}{dt} = \varpi A(t) - \nu B(t)C(t) - \rho_1 B(t) + \vartheta C(t)B(t) + \eta C(t) - \zeta \frac{C(t)}{A(t)+1}, \\ \frac{dC}{dt} = \nu C(t)B(t) - \rho_2 C(t) - \vartheta C(t)B(t) - \eta C(t) - \varkappa C(t) + \varsigma \frac{A(t)}{B(t)+1}. \end{cases} \tag{1}$$

The total amount of water $N(t) = A(t) + B(t) + C(t)$. Initial condition $A(0) = A_0$, $B(0) = B_0$ and $C(0) = C_0$. The model parameters of equation (1) are defined by Table 1.

Table 1 Model parameterization.

Parameter	Parameter Description
$A(\mathrm{t})$	Atmospheric water
$B(\mathrm{t})$	Surface water
$C(\mathrm{t})$	Groundwater
$\rho_1 \& \rho_2$	Surface and groundwater evaporation rates to atmospheric water, correspondingly
ϖ	Rate of atmospheric precipitation reaching surface water bodies
κ	Influence of surface water on atmospheric water, moderated by groundwater
ι	Rate at which atmospheric water dissipates
ν	Surface-to-groundwater infiltration rate
ϑ	The effect of pollution on groundwater and surface water
η	Recurrence rate of groundwater extraction
ζ	Reduction in surface water due to groundwater and atmospheric interaction
$\varkappa$	Pace of deforestation
ς	Contribution of atmospheric water to groundwater recharge, depending on surface water

Theorem 1. *For each non-negative initial condition, $\exists$ a unique solution of (1).*

Proof. The method utilized by Moustafa [16] is applied. The region $R = \{A(\mathrm{t}), B(\mathrm{t}), C(\mathrm{t}) \in \mathbb{R}^3_+ : |A|, |B|, |C|\}$. We use the term $T = (A, B, C)$ and $\overline{T} = (\overline{A}, \overline{B}, \overline{C})$, create a mapping

$$E(T) = (E_1(T), E_2(T), E_3(T))$$

where

$$\begin{cases} E_1(T) = \rho_1 B(\mathrm{t}) + \rho_2 C(\mathrm{t}) - \varpi A(\mathrm{t}) - \iota A(\mathrm{t}) + \kappa \frac{B(\mathrm{t})}{C(\mathrm{t})+1}, \\ E_2(T) = \varpi A(\mathrm{t}) - \nu B(\mathrm{t})C(\mathrm{t}) - \rho_1 B(\mathrm{t}) + \vartheta C(\mathrm{t})B(\mathrm{t}) + \eta C(\mathrm{t}) - \zeta \frac{C(\mathrm{t})}{A(\mathrm{t})+1}, \\ E_3(T) = \nu C(\mathrm{t})B(\mathrm{t}) - \rho_2 C(\mathrm{t}) - \vartheta C(\mathrm{t})B(\mathrm{t}) - \eta C(\mathrm{t}) - \varkappa C(\mathrm{t}) + \varsigma \frac{A(\mathrm{t})}{B(\mathrm{t})+1}. \end{cases}$$

We consider

$$\begin{aligned} ||E(T) - E(\overline{T})|| &= |E_1(T) - E_1(\overline{T})| + |E_2(T) - E_2(\overline{T})| + |E_3(T) - E_3(\overline{T})| \\ &\leq \Bigg| \rho_1 B(\mathrm{t}) + \rho_2 C(\mathrm{t}) - \varpi A(\mathrm{t}) - \iota A(\mathrm{t}) + \kappa \frac{B(\mathrm{t})}{C(\mathrm{t})+1} - \rho_1 \overline{B(\mathrm{t})} - \rho_2 \overline{C(\mathrm{t})} + \varpi \overline{A(\mathrm{t})} + \\ &\quad \iota \overline{A(\mathrm{t})} - \kappa \frac{\overline{B(\mathrm{t})}}{\overline{C(\mathrm{t})} + 1} \Bigg| + \Bigg| \varpi A(\mathrm{t}) - \nu B(\mathrm{t})C(\mathrm{t}) - \rho_1 B(\mathrm{t}) + \vartheta C(\mathrm{t})B(\mathrm{t}) + \eta C(\mathrm{t}) - \\ &\quad \zeta \frac{C(\mathrm{t})}{A(\mathrm{t})+1} - \varpi \overline{A(\mathrm{t})} + \nu \overline{B(\mathrm{t})C(\mathrm{t})} + \rho_1 \overline{B(\mathrm{t})} - \vartheta \overline{C(\mathrm{t})B(\mathrm{t})} - \eta \overline{C(\mathrm{t})} + \zeta \frac{\overline{C(\mathrm{t})}}{\overline{A(\mathrm{t})} + 1} \Bigg| \\ &\quad + \Bigg| \nu C(\mathrm{t})B(\mathrm{t}) - \rho_2 C(\mathrm{t}) - \vartheta C(\mathrm{t})B(\mathrm{t}) - \eta C(\mathrm{t}) - \varkappa C(\mathrm{t}) + \varsigma \frac{A(\mathrm{t})}{B(\mathrm{t})+1} - \nu \overline{C(\mathrm{t})B(\mathrm{t})} \\ &\quad - \rho_2 \overline{C(\mathrm{t})} - \vartheta \overline{C(\mathrm{t})B(\mathrm{t})} - \eta \overline{C(\mathrm{t})} - \varkappa \overline{C(\mathrm{t})} + \varsigma \frac{\overline{A(\mathrm{t})}}{\overline{B(\mathrm{t})} + 1} - \frac{\overline{B(\mathrm{t})}}{\overline{C(\mathrm{t})} + 1} \Bigg| \end{aligned}$$

$$
\begin{aligned}
&= |A(\mathfrak{t})-\overline{A(\mathfrak{t})}|\Big(-\iota-\frac{C(\mathfrak{t})}{(A(\mathfrak{t})+1)^2}+\frac{\zeta}{B(\mathfrak{t})+1}\Big)+|B(\mathfrak{t})-\overline{B(\mathfrak{t})}|\Big(\frac{\kappa}{C(\mathfrak{t})+1}-\\
&\quad\frac{A(\mathfrak{t})}{(B(\mathfrak{t})+1)^2}\Big)+|C(\mathfrak{t})-\overline{C(\mathfrak{t})}|\Big(-\frac{\kappa B(\mathfrak{t})}{(C(\mathfrak{t})+1)^2}-\frac{\zeta}{A(\mathfrak{t})+1}-\varkappa-\frac{\varsigma A(\mathfrak{t})}{(B(\mathfrak{t})+1)^2}\Big)\\
&\le \mathbb{C}_1|A(\mathfrak{t})-\overline{A(\mathfrak{t})}|+\mathbb{C}_2|B(\mathfrak{t})-\overline{B(\mathfrak{t})}|+\mathbb{C}_3|C(\mathfrak{t})-\overline{C(\mathfrak{t})}|\\
&\le \mathbb{C}_{max}|F-\overline{F}|,
\end{aligned}
$$

where $\mathbb{C}_{max}=max\{\mathbb{C}_1,\mathbb{C}_2,\mathbb{C}_3\}$.

As a result, we deduce that the $+^{vely}$ invariant set induced by the model (1) is the area R. In the region R, the model is well-posed both mathematically and biologically. Thus, the existence criterion of the system (1) is established.

Theorem 2. *The solution of system (1) which start in R^3_+ are uniformly bounded and non-negative.*

Proof. Since the total amount of water is $N(\mathfrak{t})=A(\mathfrak{t})+B(\mathfrak{t})+C(\mathfrak{t})$, the rate of change of the water content $N(\mathfrak{t})$,

$$
\begin{aligned}
\frac{dN}{d\mathfrak{t}} &= \frac{dA}{d\mathfrak{t}}+\frac{dB}{d\mathfrak{t}}+\frac{dC}{d\mathfrak{t}}\\
&= \rho_1 B(\mathfrak{t})+\rho_2 C(\mathfrak{t})-\varpi A(\mathfrak{t})-\iota A(\mathfrak{t})+\kappa\frac{B(\mathfrak{t})}{C(\mathfrak{t})+1}+\varpi A(\mathfrak{t})-\nu B(\mathfrak{t})C(\mathfrak{t})-\rho_1 B(\mathfrak{t})\\
&\quad+\vartheta C(\mathfrak{t})B(\mathfrak{t})+\eta C(\mathfrak{t})-\zeta\frac{C(\mathfrak{t})}{A(\mathfrak{t})+1}+\nu C(\mathfrak{t})B(\mathfrak{t})-\rho_2 C(\mathfrak{t})-\vartheta C(\mathfrak{t})B(\mathfrak{t})-\eta C(\mathfrak{t})\\
&\quad-\varkappa C(\mathfrak{t})+\varsigma\frac{A(\mathfrak{t})}{B(\mathfrak{t})+1}\\
&\le -\iota A(\mathfrak{t})-\varkappa C(\mathfrak{t})+\kappa\frac{B(\mathfrak{t})}{C(\mathfrak{t})+1}-\zeta\frac{C(\mathfrak{t})}{A(\mathfrak{t})+1}+\varsigma\frac{A(\mathfrak{t})}{B(\mathfrak{t})+1}.
\end{aligned}
$$

This implies that $\frac{dN}{d\mathfrak{t}}$ is bounded above and below by terms involving $-(\iota A(\mathfrak{t})+\varkappa C(\mathfrak{t}))$. Integrating the above inequality and using initial conditions, we obtain

$$
N(0)e^{(\iota+\varkappa)\mathfrak{t}}\le N(\mathfrak{t})\le N(0)e^{(\iota+\varkappa)\mathfrak{t}}.
$$

Considering $t\to\infty$, we have

$$
\lim_{\mathfrak{t}\to\infty} infN(\mathfrak{t})\le N(\mathfrak{t})\le \lim_{\mathfrak{t}\to\infty} supN(\mathfrak{t}).
$$

Hence the feasible region for the system (1) is

$$
R=\{A(\mathfrak{t}),B(\mathfrak{t}),C(\mathfrak{t})\in\mathbb{R}^3_+ : 0<|A|,|B|,|C|\le N(0)e^{(\iota+\varkappa)t}\}.
$$

Hence the region R is positive invariant so that no solution path moves beyond the boundary of R. Thus above theorem ensures that the proposed model is feasible both biologically and mathematically.

3 Results of equilibrium

In order to identify the model's equilibrium points (1), we must solve

$$
\frac{dA}{d\mathfrak{t}}=\frac{dB}{d\mathfrak{t}}=\frac{dC}{d\mathfrak{t}}=0.
$$

The system then assumes the subsequent configuration

$$\begin{cases} \rho_1 B(\mathrm{t}) + \rho_2 C(\mathrm{t}) - \varpi A(\mathrm{t}) - \iota A(\mathrm{t}) + \kappa \frac{B(\mathrm{t})}{C(\mathrm{t})+1} = 0, \\ \varpi A(\mathrm{t}) - \nu B(\mathrm{t})C(\mathrm{t}) - \rho_1 B(\mathrm{t}) + \vartheta C(\mathrm{t})B(\mathrm{t}) + \eta C(\mathrm{t}) - \zeta \frac{C(\mathrm{t})}{A(\mathrm{t})+1} = 0, \\ \nu C(\mathrm{t})B(\mathrm{t}) - \rho_2 C(\mathrm{t}) - \vartheta C(\mathrm{t})B(\mathrm{t}) - \eta C(\mathrm{t}) - \varkappa C(\mathrm{t}) + \varsigma \frac{A(\mathrm{t})}{B(\mathrm{t})+1} = 0. \end{cases} \tag{2}$$

1. When it comes to pollution-free and groundwater-free pumping, we consider $B = B_0$.
   Let $\overline{E}_1(\overline{A(\mathrm{t})}, \overline{B(\mathrm{t})}, \overline{C(\mathrm{t})})$ be the pollution free equilibrium point. Using $B = B_0$ in the system (2), and solving the system of algebraic equation, we obtain

$$\overline{A(\mathrm{t})} = \frac{\rho_1 B_0(\mathrm{t}) + \rho_2 \overline{C(\mathrm{t})} + \frac{\kappa B_0(\mathrm{t})}{C(\mathrm{t})+1}}{\varpi + \iota},$$

   and

$$\overline{C(\mathrm{t})}[\nu B(\mathrm{t}) - \rho_2 - \vartheta B(\mathrm{t}) - \varkappa - \eta] = -\frac{\varsigma \overline{A(\mathrm{t})}}{B(\mathrm{t})+1},$$
$$\overline{C(\mathrm{t})} = \frac{\varkappa \overline{A(\mathrm{t})}}{(B(\mathrm{t})+1)(\rho_2 + \vartheta B_0 + \eta + \varkappa - \nu B_0)}.$$

2. The Atmospheric-Surface water equilibrium point $E_2 = (A(t), B(t), 0)$ where

$$\rho_1 B(\mathrm{t}) - \varpi A(\mathrm{t}) - \iota A(\mathrm{t}) + \kappa B(\mathrm{t}) = 0,$$
$$(\varpi + \iota)A(\mathrm{t}) - (\rho_1 + \kappa)B(\mathrm{t}) = 0,$$
$$A(\mathrm{t}) = \frac{(\rho_1 + \kappa)B(\mathrm{t})}{\varpi + \iota}.$$

3. The Atmospheric-Ground water equilibrium point $E_3 = (A(\mathrm{t}), 0, C(\mathrm{t}))$,

$$\rho_2 C(\mathrm{t}) - \varpi A(\mathrm{t}) - \iota A(\mathrm{t}) = 0,$$
$$C(\mathrm{t}) = \frac{\varpi + \iota}{\rho_2} A(\mathrm{t}).$$

4. The Surface- Ground water equilibrium point $E_4 = (0, B(\mathrm{t}), C(\mathrm{t}))$,

$$\nu C(\mathrm{t})B(\mathrm{t}) - \rho_2 C(\mathrm{t}) - \vartheta C(\mathrm{t})B(\mathrm{t}) - \eta C(\mathrm{t}) - \varkappa C(\mathrm{t}) = 0,$$
$$B(\mathrm{t})C(\mathrm{t})(\nu - \vartheta) = C(\mathrm{t})(\rho_2 + \eta + \varkappa),$$
$$B(\mathrm{t}) = \frac{\rho_2 + \eta + \varkappa}{\nu - \vartheta}.$$

4 The local stability of steady state points

The stability criteria of the possible stable state points are described as follows.

Theorem 3. *The steady state point E_0 is conditionally locally asymptotically stable if the following condition satisfied $\rho_1 < \kappa$ [36].*

Proof. At E_0, the Jacobian matrix for (1) is given by

$$J(A,B,C)=\begin{pmatrix} -\iota-\varpi & \rho_1+\frac{\kappa}{C(\mathrm{t})+1} & \rho_2-\frac{\kappa B(\mathrm{t})}{(C(\mathrm{t})+1)^2} \\ \varpi-\frac{\zeta C(\mathrm{t})}{(A(\mathrm{t})+1)^2} & -\nu C(\mathrm{t})-\rho_1+\vartheta C(\mathrm{t}) & -\nu B(\mathrm{t})+\vartheta B(\mathrm{t})+\eta-\frac{\zeta}{A(\mathrm{t})+1} \\ \frac{\varsigma}{B(\mathrm{t})+1} & \nu C(\mathrm{t})-\vartheta C(\mathrm{t})-\frac{\varsigma A(\mathrm{t})}{(B(\mathrm{t})+1)^2} & \nu B(\mathrm{t})-\rho_2-\vartheta B(\mathrm{t})-\eta-\varkappa \end{pmatrix}$$

$$J(E_0)=\begin{pmatrix} -(\iota+\varpi) & \rho_1+\kappa & \rho_2-\kappa B(\mathrm{t}) \\ \varpi & -\rho_1 & -(\eta+\zeta) \\ 0 & 0 & -(\rho_2+\eta+\varkappa) \end{pmatrix}$$

$(\lambda_1-a_{33})(\lambda^2-(a_{11}+a_{22})\lambda+(a_{11}a_{22}-a_{12}a_{21}))=0.$
The characteristic polynomial of $J(E_0)$ is $(\lambda_1+\rho_2+\eta+\varkappa)((\lambda^2+\lambda(\iota+\varpi+\rho_1)+(\iota+\varpi)\rho_1-\varpi(\rho_1+\kappa))=0$.
It's observed that all roots of the characteristic polynomial of $J(E_0)$ is equation have a $-^{ve}$ real part, $\rho_1<\kappa$.

Theorem 4. *The steady point E_1 is conditionally asymptotically stable if the following conditions are satisfied $\kappa B(\mathrm{t})>\rho_2, \frac{\zeta}{A(\mathrm{t})+1}+\nu B(\mathrm{t})>\vartheta B(\mathrm{t})+\eta$ and $\vartheta B(\mathrm{t})+\eta+\varkappa+\rho_2>\nu B(\mathrm{t})$.*

Proof. At E_1, then Jacobian matrix of (1) is,

$$J(E_1)=\begin{pmatrix} -(\iota+\varpi) & \rho_1+\kappa & \rho_2-\kappa B(\mathrm{t}) \\ \varpi & -\rho_1 & -\nu B(\mathrm{t})+\vartheta B(\mathrm{t})+\eta-\frac{\zeta}{A(\mathrm{t})+1} \\ \frac{\varsigma}{B(\mathrm{t})+1} & \frac{-\varsigma A(\mathrm{t})}{(B(\mathrm{t})+1)^2} & \nu B(\mathrm{t})-\rho_2-\vartheta B(\mathrm{t})-\eta-\varkappa \end{pmatrix}$$

$\lambda^3-[a_{11}+a_{22}+a_{33}]\lambda^2+[a_{22}a_{33}-a_{23}a_{32}+a_{11}a_{33}-a_{31}a_{13}+a_{11}a_{22}-a_{12}a_{21}]\lambda$ $-a_{11}[a_{22}a_{33}-a_{23}a_{32}]+a_12[a_{21}a_{33}-a_{23}a_{31}]-a_{13}[a_{21}a_{32}-a_{31}a_{22}]=0$ when we examine the element of Jacobian matrix, we can see that the signs of elements a_{11},a_{22} and a_{32} are strictly $-^{ve}$, while the signs of elements a_{12},a_{21} and a_{31} are strictly $+^{ve}$. On the other hand the signs of elements a_{13},a_{23} and a_{33} have $-^{ve}$ signs provided that $\kappa B(\mathrm{t})>\rho_2, \frac{\zeta}{A(\mathrm{t})+1}+\nu B(\mathrm{t})>\vartheta B(\mathrm{t})+\eta$ and $\vartheta B(\mathrm{t})+\eta+\varkappa+\rho_2>\nu B(\mathrm{t})$ respectively.

Theorem 5. *The steady state point E_2 is conditionally asymptotically stable if the following conditions are satisfied $\frac{\zeta C(\mathrm{t})}{(A(\mathrm{t})+1)^2}>\varpi, \nu C(\mathrm{t})+\rho_1>\vartheta C(\mathrm{t}), \frac{\zeta}{A(\mathrm{t})+1}>\eta$ and $\vartheta C(\mathrm{t})+\varsigma A(\mathrm{t})>\nu C(\mathrm{t})$.*

Proof. At E_2, then Jacobian matrix of (1) is given by,
$J(E_2)=[Jij]_{i,j}=1,2,3.$

$$J(E_2)=\begin{pmatrix} -(\iota+\varpi) & \rho_1+\frac{\kappa}{C(\mathrm{t})+1} & \rho_2 \\ \varpi-\frac{\zeta C(\mathrm{t})}{(A(\mathrm{t})+1)^2} & -\nu C(\mathrm{t})-\rho_1+\vartheta C(\mathrm{t}) & \eta-\frac{\zeta}{A(\mathrm{t})+1} \\ \varsigma & \nu C(\mathrm{t})-\vartheta C(\mathrm{t})-\varsigma A(\mathrm{t}) & -(\rho_2+\eta+\varkappa) \end{pmatrix}$$

$$\begin{aligned}&\mathscr{A}_1=-(a_{11}+a_{22}+a_{33}), \mathscr{A}_2=-a_{22}a_{33}+a_{23}a_{32}-a_{11}a_{33}+a_{31}a_{13}-a_{11}a_{22}+a_{21}a_{12},\\ &\mathscr{A}_3=-a_{11}a_{22}a_{33}+a_{11}a_{23}a_{32}-a_{12}a_{21}a_{33}+a_{12}a_{23}a_{31}-a_{31}a_{21}a_{32}+a_{13}a_{31}a_{22},\end{aligned}$$

when we analyze the components of the Jacobian matrix, we notice that a_{11} and a_{33} have strictly negative signs, whereas a_{21},a_{22},a_{23} and a_{32} have negative sign provided that $\frac{\zeta C(\mathrm{t})}{(A(\mathrm{t})+1)^2}>\varpi, \nu C(\mathrm{t})+\rho_1>\vartheta C(\mathrm{t}), \frac{\zeta}{A(\mathrm{t})+1}>\eta$ and $\vartheta C(\mathrm{t})+\varsigma A(\mathrm{t})>\nu C(\mathrm{t})$ respectively.

Under the specified criteria, A_1,A_3 and $A_1A_2>A_3$ are all positive signals.
Now, let

$$\mathscr{A}_2(\mathfrak{Y})=\mathfrak{Y}^3+\mathscr{A}_1\mathfrak{Y}^2+\mathscr{A}_2\mathfrak{Y}+\mathscr{A}_3.$$

Thus, this polynomial's discriminant is

$$D(\mathscr{A}_2) = 18\mathscr{A}_1\mathscr{A}_2\mathscr{A}_3 + (\mathscr{A}_1\mathscr{A}_2)^2 - 4\mathscr{A}_3\mathscr{A}_1^3 - 4\mathscr{A}_2^3 - 27\mathscr{A}_3^2.$$

Matignon's criteria and the Routh-Hurwitz criterion state that the equilibrium point E_2 is locally asymptotically stable if $\frac{\zeta C(\mathrm{t})}{(A(\mathrm{t})+1)^2} > \varpi, \nu C(\mathrm{t}) + \rho_1 > \vartheta C(\mathrm{t}), \frac{\zeta}{A(\mathrm{t})+1} > \eta, \vartheta C(\mathrm{t}) + \varsigma A(\mathrm{t}) > \nu C(\mathrm{t})$ and $D_2(A_2) > 0$.

Theorem 6. *The steady state point E_3 is conditionally asymptotically stable if the following conditions are satisfied $\frac{\kappa B(\mathrm{t})}{(C(\mathrm{t})+1)^2} > \rho_2, \nu C(\mathrm{t}) + \rho_1 > \vartheta C(\mathrm{t}), \nu B(\mathrm{t}) + \frac{\zeta}{A(\mathrm{t})+1} > \vartheta B(\mathrm{t}) + \eta, \vartheta C(\mathrm{t}) + \frac{\varsigma A(\mathrm{t})}{(B(\mathrm{t})+1)^2} > \nu C(\mathrm{t})$ and $\rho_2 + \vartheta B(\mathrm{t}) + \eta + \varkappa > \nu B(\mathrm{t})$.*

Proof. At E_3, Jacobian matrix for (1), we have

$$J(E_3) = \begin{pmatrix} -(\iota+\varpi) & \rho_1 + \frac{\kappa}{C(\mathrm{t})+1} & \rho_2 - \frac{\kappa B(\mathrm{t})}{(C(\mathrm{t})+1)^2} \\ \varpi - \frac{\zeta C(\mathrm{t})}{(A(\mathrm{t})+1)^2} & -\nu C(\mathrm{t}) - \rho_1 + \vartheta C(t) & -\nu B(\mathrm{t}) + \vartheta B(\mathrm{t}) + \eta - \frac{\zeta}{A(\mathrm{t})+1} \\ \frac{\varsigma}{B(\mathrm{t})+1} & \nu C(\mathrm{t}) - \vartheta C(\mathrm{t}) - \frac{\varsigma A(\mathrm{t})}{(B(\mathrm{t})+1)^2} & \nu B(\mathrm{t}) - \rho_2 - \vartheta B(\mathrm{t}) - \eta - \varkappa \end{pmatrix}$$

where

$$\begin{aligned} &\mathfrak{Y}^3 + \mathscr{A}_1\mathfrak{Y}^2 + \mathscr{A}_2\mathfrak{Y} + \mathscr{A}_3 = 0 \\ &\mathscr{A}_1 = -(a_{11} + a_{22} + a_{33}), \mathscr{A}_2 = -a_{11}a_{33} + a_{23}a_{32} - a_{11}a_{33} + a_{31}a_{13} - a_{11}a_{22} + a_{21}a_{12}, \\ &\mathscr{A}_3 = -a_{11}a_{22}a_{33} + a_{11}a_{23}a_{32} - a_{12}a_{21}a_{33} + a_{12}a_{23}a_{31} - a_{31}a_{21}a_{32} + a_{13}a_{31}a_{22}. \end{aligned}$$

Sign of element a_{11} strictly negative, while the sign of elements a_{12}, a_{21} and a_{31} strictly positive. The sign of elements $a_{13}, a_{22}, a_{23}, a_{32}$ and a_{33} are negative provided that $\frac{\kappa B(\mathrm{t})}{(C(\mathrm{t})+1)^2} > \rho_2, \nu C(\mathrm{t}) + \rho_1 > \vartheta C(\mathrm{t}), \nu B(\mathrm{t}) + \frac{\zeta}{A(\mathrm{t})+1} > \vartheta B(\mathrm{t}) + \eta, \vartheta C(\mathrm{t}) + \frac{\varsigma A(\mathrm{t})}{(B(\mathrm{t})+1)^2} > \nu C(\mathrm{t})$ and $\rho_2 + \vartheta B(\mathrm{t}) + \eta + \varkappa > \nu B(\mathrm{t})$, respectively.

Theorem 7. *The steady state point E_4 is conditionally asymptotically stable if the following conditions are satisfied $\frac{\kappa B(\mathrm{t})}{(C(\mathrm{t})+1)^2} > \rho_2, \zeta C(\mathrm{t}) > \varpi, \nu C(\mathrm{t}) + \rho_1 > \vartheta C(\mathrm{t}), \nu B(\mathrm{t}) + \zeta > \vartheta B(\mathrm{t}) + \eta, \vartheta C(\mathrm{t}) > \nu C(\mathrm{t})$ and $\rho_2 + \vartheta B(\mathrm{t}) + \eta + \varkappa > \nu B(\mathrm{t})$.*

Proof. At E_4, Jacobian matrix for (1), we have

$$J(E_4) = \begin{pmatrix} -(\iota+\varpi) & \rho_1 + \frac{\kappa}{C(\mathrm{t})+1} & \rho_2 - \frac{\kappa B(\mathrm{t})}{(C(\mathrm{t})+1)^2} \\ \varpi - \zeta C(\mathrm{t}) & -\nu C(\mathrm{t}) - \rho_1 + \vartheta C(t) & -\nu B(\mathrm{t}) + \vartheta B(\mathrm{t}) + \eta - \zeta \\ \frac{\varsigma}{B(\mathrm{t})+1} & \nu C(\mathrm{t}) - \vartheta C(\mathrm{t}) & \nu B(\mathrm{t}) - \rho_2 - \vartheta B(\mathrm{t}) - \eta - \varkappa \end{pmatrix}$$

$$\begin{aligned} &\mathfrak{Y}^3 + \mathscr{A}_1\mathfrak{Y}^2 + \mathscr{A}_2\mathfrak{Y} + \mathscr{A}_3 = 0 \\ \text{where} \quad &\mathscr{A}_1 = -(a_{11} + a_{22} + a_{33}), \mathscr{A}_2 = -a_{11}a_{33} + a_{23}a_{32} - a_{11}a_{33} + a_{31}a_{13} - a_{11}a_{22} + a_{21}a_{12}, \\ &\mathscr{A}_3 = -a_{11}a_{22}a_{33} + a_{11}a_{23}a_{32} - a_{12}a_{21}a_{33} + a_{12}a_{23}a_{31} - a_{31}a_{21}a_{32} + a_{13}a_{31}a_{22}. \end{aligned}$$

Sign of element a_{11} strictly negative, while the sign of elements a_{12} and a_{31} strictly positive. The sign of elements $a_{13}, a_{21}, a_{22}, a_{23}, a_{32}$ and a_{33} are negative provided that $\frac{\kappa B(\mathrm{t})}{(C(\mathrm{t})+1)^2} > \rho_2, \zeta C(\mathrm{t}) > \varpi, \nu C(\mathrm{t}) + \rho_1 > \vartheta C(\mathrm{t}), \nu B(\mathrm{t}) + \zeta > \vartheta B(\mathrm{t}) + \eta, \vartheta C(\mathrm{t}) > \nu C(\mathrm{t})$ and $\rho_2 + \vartheta B(\mathrm{t}) + \eta + \varkappa > \nu B(\mathrm{t})$, respectively.

5 Numerical simulation

In this section, we implement a numerical simulation using RK4 to solve a system of ODEs representing the interactions between atmospheric water (A), surface water (B), and groundwater (C). The parameter values are taken from [1] and the values of κ, ζ and ς scale proportionally without causing unbounded effects, resulting in a stable and realistic model. The model incorporates key environmental factors such as precipitation, evaporation, infiltration, deforestation, pollution, and water pumping. Additionally, new terms are added to capture the dynamic interactions between these water bodies.

Through the numerical simulation, we validate the model by observing how these parameters influence the stability, equilibrium points, and overall behavior of the water system under various scenarios.

Table 2 Model parameterization with values.

Parameter	Parameter Description	Parameter Value
$\rho_1 \& \rho_2$	Surface and groundwater evaporation rates to atmospheric water, correspondingly	0.09 & 0.028
ϖ	Precipitation rate from atmosphere to surface water	0.5
κ	Influence of surface water on atmospheric water, modereted by groundwater	0.05
ι	Rate at which atmospheric water dissipates	0.01
ν	Surface-to-groundwater infiltration rate	0.3005
ϑ	The effect of pollution on groundwater and surface water	0.300
η	Recurrence rate of groundwater extraction	0.02
ζ	Reduction in surface water due to groundwater and atmospheric interaction	0.07
$\varkappa$	Pace of deforestation	0.06
ς	Contribution of atmospheric water to groundwater recharge, depending on surface water	0.04

The proposed model is solved using the classical RK4 method due to its accuracy and stability for nonlinear systems. The model equations are implemented in MATLAB with a fixed time step h=0.01. To ensure robustness, selected results are cross-validated using a shifted Jacobi spectral method, confirming consistency with existing approaches such as those by Ebrahimzadeh et al. [32]. The parameters used in this simulation are summarized in Table 2, with values derived from the data presented in Table 1.

Figure 1 shows how precipitation, dissipation, and evaporation from surface and groundwater transform atmospheric water levels throughout time. Figure 2 shows how precipitation, groundwater penetration, evaporation, and pollution affect surface water levels. Associations with groundwater have had a significant role in surface water changes. Figure 3 illustrates groundwater dynamics, including effects from infiltration, evaporation, deforestation, and water extraction. The mathematical model shows that, while air and surface water levels are declining owing to evaporation and pollution, groundwater levels remain steady. This stability can serve as a buffer against sudden changes in surface and atmospheric water. However, persistent losses in surface and atmospheric water might jeopardise long-term groundwater recharge and sustainability, especially with rising pollution and deforestation.

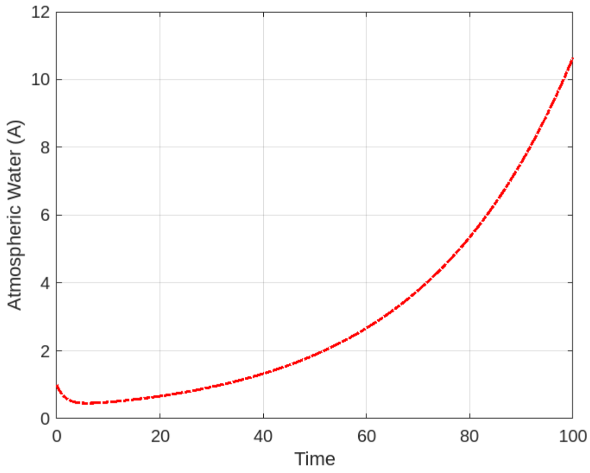

Fig. 1 Atmospherical water.

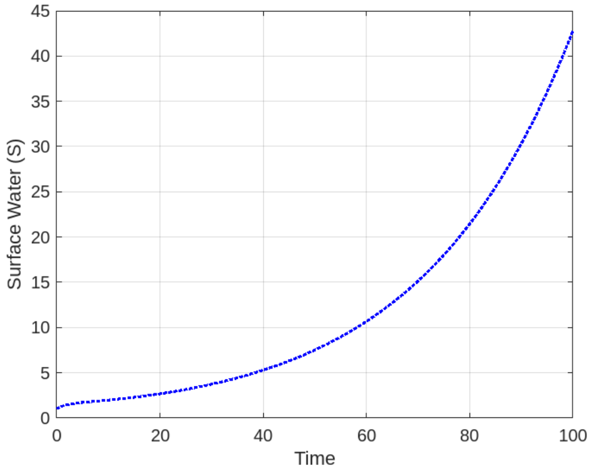

Fig. 2 Surface water.

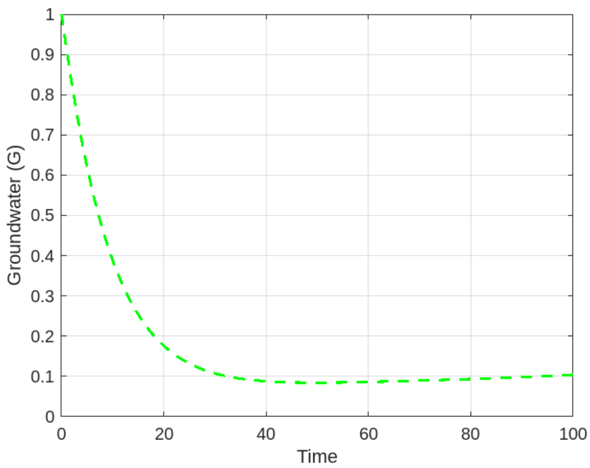

Fig. 3 The groundwater.

6 Results and discussion

The numerical simulations conducted for the proposed ODE model reveal key dynamics in the interaction between atmospheric water (A), surface water (S), and groundwater (C) compartments. The solutions show that under baseline conditions, the groundwater level tends to stabilize after initial fluctuations, indicating the system's inherent stability. However, the inclusion of anthropogenic factors such as deforestation and frequent pumping shifts the equilibrium, resulting in long-term groundwater depletion. Among all parameters, the groundwater recharge rate and deforestation parameter had the most significant influence on groundwater dynamics, as demonstrated by the sharper decline in C over time when these values increased. These results emphasize the critical importance of preserving forest cover and regulating water extraction.

7 Conclusion

Groundwater is essential to preserving natural equilibrium and enabling human activity. However, it is increasingly threatened by factors like pollution, overconsumption, and deforestation. To address these challenges, we have developed an advanced ODE model that integrates new terms to represent the complex interactions between atmospheric water, surface water, and groundwater. Through the analysis of equilibrium points, stability, and numerical simulations, we validated the model's accuracy across diverse scenarios. The numerical simulations, which are confirmed by the figures, disclose numerous important results. They illustrated that surface and atmospheric water levels decrease over time caused by pollution and evaporation, although groundwater remains rather steady in the near term. However, continuous environmental stressors gradually reduce groundwater recharge, highlighting underground water systems' delayed but vital vulnerability. Compared to prior models that address various water sources in isolation or without environmental coupling, our model provides a more integrated and adaptable framework. This integration broadens its application in measuring water sustainability and implementing more effective groundwater management techniques.

The novelty and contribution of this paper are the following:

- We extended an existing ODE-based water cycle model by introducing new nonlinear terms that reflect moderated interactions between atmospheric, surface, and groundwater.
- The extended model captures complex interdependencies within the hydrological system more realistically than previous formulations.
- We conducted equilibrium and stability analysis, and validated the model using numerical simulations under varying environmental conditions.

The model provides a foundational tool for assessing the long-term impacts of environmental changes and can be extended in future work for scenario analysis under varying climate and land-use conditions.

8 Declarations

8.1 Conflict of interest:

The authors hereby declare that there is no conflict of interests regarding the publication of this paper.

8.2 Funding:

No funding was received to assist with the preparation of this manuscript.

8.3 Author's contribution:

K.S.N.-Conceptualization, Formal Analysis, Methodology, Software, Writing–Original Draft. R.M.A. and M.S.A.-Investigation, Methodology, Software, Investigation, Validation. Finally, all authors read and approved the last published version of the manuscript.

8.4 Acknowledgement:

This study is supported via funding from Prince Sattam bin Abdulaziz University project number (PSAU/2025/R/1446).

8.5 Data availability statement:

All data that support the findings of this study are included within the article.

8.6 Usage of AI tools:

The authors declare that they have not used Artificial Intelligence (AI) tools in the creation of this article.

References

[1] Islam M.A., Biswas M.H.A., Potential impact of climate change on groundwater level declination in Bangladesh: A mathematical modeling computation, Informatica, 47(2), 261–274, 2023.

[2] Thirthar A.A., Panja P., Majeed S.J., Nisar K.S., Dynamic interactions in a two-species model of the mammalian predator-prey system: The influence of Allee effects, prey refuge, water resources, and moonlights, Partial Differential Equations in Applied Mathematics, 11, 100865, 2024.

[3] Thirthar A.A., Jawad S., Majeed S.J., Nisar K.S., Impact of wind flow and global warming in the dynamics of prey-predator model, Results in Control and Optimization, 15, 100424, 2024.

[4] Al-Qubatee W., Hasan F.A., Ritzema H., Nasher G., Hellegers P., Natural and human-induced drivers of groundwater depletion in Wadi Zabid, Tihama coastal plain, Yemen, Journal of Environmental Planning and Management, 65(14), 2609–2630, 2022.

[5] Mandal S., Islam M.S., Biswas M.H.A., Akter S., A mathematical model applied to investigate the potential impact of global warming on marine ecosystems, Applied Mathematical Modelling, 101, 19–37, 2022.

[6] World Bank, Chart: Globally, 70% of freshwater is used in agriculture, https://blogs.worldbank.org/en/opendata/chart-globally-70-freshwater-used-agriculture, Accessed: January 01, 2026.

[7] NGWA, Information on Earth's Water, https://www.ngwa.org/what-is-groundwater/About-groundwater/information-on-earths-wate, Accessed: January 01, 2026.

[8] NGWA, Get involved: Groundwater Awareness Week, https://www.ngwa.org/get-involved/gwaw, Accessed: January 01, 2026.

[9] Amanambu A.C., Obarein O.A., Mossa J., Li L., Ayeni S.S., Balogun O., Oyebamiji A., Ochege F.U., Groundwater system and climate change: Present status and future considerations, Journal of Hydrology, 589, 125163, 2020.

[10] Davamani V., John J.E., Poornachandhra C., Gopalakrishnan B., Arulmani S., Parameswari E., Santhosh A., Srinivasulu A., Lal A., Naidu R., A critical review of climate change impacts on groundwater resources: A focus on the current status, future possibilities, and role of simulation models, Atmosphere, 15(1), 122, 2024.

[11] NOAA, Climate change: Atmospheric carbon dioxide, https://www.climate.gov/news-features/understanding-climate/climate-change-atmospheric-carbon-dioxide, Accessed: January 01, 2026.

[12] Nisar K.S., Logeswari K., Vijayaraj V., Baskonus H.M., Ravichandran C., Fractional order modeling the Gemini virus in Capsicum annuum with optimal control, Fractal and Fractional, 6(2), 61, 2022.

[13] Elsonbaty A., Adel W., Sabbar Y., El-Mesady A., Nonlinear dynamics and optimal control of a fractional order cotton leaf curl virus model incorporating climate change influences, Partial Differential Equations in Applied Mathematics, 10, 100727, 2024.

[14] Singh J., Agrawal R., Nisar K.S., A new forecasting behavior of fractional model of atmospheric dynamics of carbon dioxide gas, Partial Differential Equations in Applied Mathematics, 9, 100595, 2024.

[15] Nisar K.S., Farman M., Abdel-Aty M., Ravichandran C., A review of fractional order epidemic models for life sciences problems: Past, present and future, Alexandria Engineering Journal, 95, 283–305, 2024.

[16] Moustafa M., Dynamical analysis of a fractional-order Rosenzweig-MacArthur model incorporating a prey refuge,

Chaos Solitons & Fractals, 109, 1–13, 2018.
[17] Ravichandran C., Logeswari K., Khan A., Abdeljawad T., Gómez-Aguilar J.F., An epidemiological model for computer virus with Atangana-Baleanu fractional derivative, Results in Physics, 51, 106601, 2023.
[18] Nisar K.S., Farman M., Abdel-Aty M., Ravichandran C., A review of fractional-order models for plant epidemiology, Progress in Fractional Differentiation and Applications, 10(3), 489–521, 2024.
[19] Maji C., Basir F.A., Mukherjee D., Nisar K.S., Ravichandran C., COVID-19 propagation and the usefulness of awareness-based control measures: A mathematical model with delay, AIMS Mathematics, 7(7), 12091–12105, 2022.
[20] Ravichandran C., Trujillo J.J., Controllability of impulsive fractional functional integro-differential equations in banach spaces, Journal of Function Spaces, 2013(1), 812501, 2013.
[21] Baalousha H.M., Barth N., Ramasomanana F.H., Ahzi S., Groundwater recharge estimation and its spatial distribution in arid regions using GIS: A case study from Qatar karst aquifer, Modeling Earth Systems and Environment, 4(4), 1319–1329, 2018.
[22] Bear J., Verruijt A., Modeling Groundwater Flow and Pollution, Theory and Applications of Transport in Porous Media, D.Reidel Publishing Company, Holland, 1998.
[23] Brammer H., Ravenscroft P., Arsenic in groundwater: A threat to sustainable agriculture in South and South-east Asia, Environment International, 35(3), 647–654, 2009.
[24] Brenner S., Coxon G., Nicholas J.K.H., Freer J., Hartmann A., Process-based modelling to evaluate simulated groundwater levels and frequencies in a Chalk catchment in south-western England, Natural Hazards and Earth System Sciences, 18(2), 445–461, 2018.
[25] Brouyére S., Carabin G., Dassargues A., Climate change impacts on groundwater resources: modelled deficits in a chalky aquifer, Geer Basin, Belgium, Hydrogeology Journal, 12, 123–134, 2004.
[26] Burghes D.N., Borrie M.S., Modeling with Differential Equations, Ellis Horwood Series, John Wiley & Sons, New York, USA, 1981.
[27] Mandal S., Islam M.S., Biswas M.H.A., Modeling the potential impact of climate change on living beings near coastal area, Modeling Earth Systems and Environment, 7, 1783–1796, 2021.
[28] Wieland M., Arne W., Marheineke N., Weger R., Modeling and simulation of curved fibers in dry spinning scenarios, Results in Applied Mathematics, 3, 100013, 2019.
[29] Parvin M., The rate of decline and trend line analysis of groundwater underneath Dhaka and Gazipur City, Journal of Water Resource and Protection, 11(3), 348–356, 2019.
[30] Shukla J.B., Arora M.S., Verma M., Misra A.K., Takeuchi Y., The impact of sea level rise due to global warming on the coastal population dynamics: A modeling study, Earth Systems and Environment, 5, 909–926, 2021.
[31] Piccolroaz S., Zhu S., Ladwig R., Carrea L., Oliver S., Piotrowski A.P., Ptak M., Shinohara R., Sojka M., Woolway R.I., Zhu D.Z., Lake water temperature modeling in an era of climate change: Data sources, models, and future prospects, Reviews of Geophysics, 62(1), e2023RG000816, 2024.
[32] Ebrahimzadeh A., Hashemizadeh E., Mirabbasi R., A numerical solution of the mathematical models for water pollution by shifted Jacobi polynomials, TWMS Journal of Applied and Engineering Mathematics, 15(2), 298–308, 2025.
[33] Bhavithra H.A., Kiruthika N., Devi S.S., Sustainable Environmental Remediation: Avenues in Nano and Biotechnology, (Chapter: Mathematical modelling to control the spread of water contamination of uppanar river in Cuddalore district), 521–541, 2025.
[34] Garcia R.O., Silveira G.P., Numerical simulation of Saint-Venant equations with thermal energy dependency: Applications on global warming, Open Journal of Fluid Dynamics, 13(4), 191–205, 2023.
[35] Farman M., Shehzad A., Nisar K.S., Hincal E., Akgul A., Hassan A.M., Generalized Ulam-Hyers-Rassias stability and novel sustainable techniques for dynamical analysis of global warming impact on ecosystem, Scientific Reports, 13(1), 22441, 2023.
[36] Majeed S.J., Naji R.K., Thirthar A.A., The dynamics of an omnivore-predator-prey model with harvesting and two different nonlinear functional responses, AIP Conference Proceedings, 2096(020008), 2019.